



Finding Atmospheres on M-Dwarf Terrestrial Planets

Megan Mansfield¹, Daniel Koll², Matej Malik³, Eliza M.-R. Kempton³, Edwin S. Kite¹, Jacob L. Bean⁴, Dorian Abbot¹, Renyu Hu⁵ ¹University of Chicago, Department of Geophysical Sciences; ²Massachusetts Institute of Technology, Department of Earth, Atmospheric and Planetary Sciences; ³University of Maryland, Department of Astronomy; ⁴University of Chicago, Department of Astronomy & Astrophysics; ⁵California Institute of Technology, Jet Propulsion Laboratory

Motivation

- XUV flux of M dwarfs may be strong enough to strip atmospheres [e.g. 1]
- Habitability of planets observable by JWST depends on whether they can retain atmospheres
- 2 main goals explored in 4 papers:
 - New atmospheric modeling of terrestrial M-dwarf planets
 - New observational tests for presence/absence of atmospheres
- Focus on 3 canonical planets with a range of temperatures: GJ 1132b [2], TRAPPIST-1b [3], and LHS 3844b [4]

1D Modeling (Malik et al., submitted)

- 1D models of planets using HELIOS [5,6] in radiative-convective equilibrium using self-consistent temperature-pressure (T-P) profiles
- Included effect of solid surface for the first time
- 3 atmosphere compositions explored: solar, pure H₂O, pure CO₂
- M-dwarf emission in near-infrared → H₂O and CO₂ absorb incoming light in upper atmosphere
 - Less heating near surface → inhibits convection
 - Thermal inversion possible (especially for cool planets with lower-altitude photospheres; Fig. 1)**

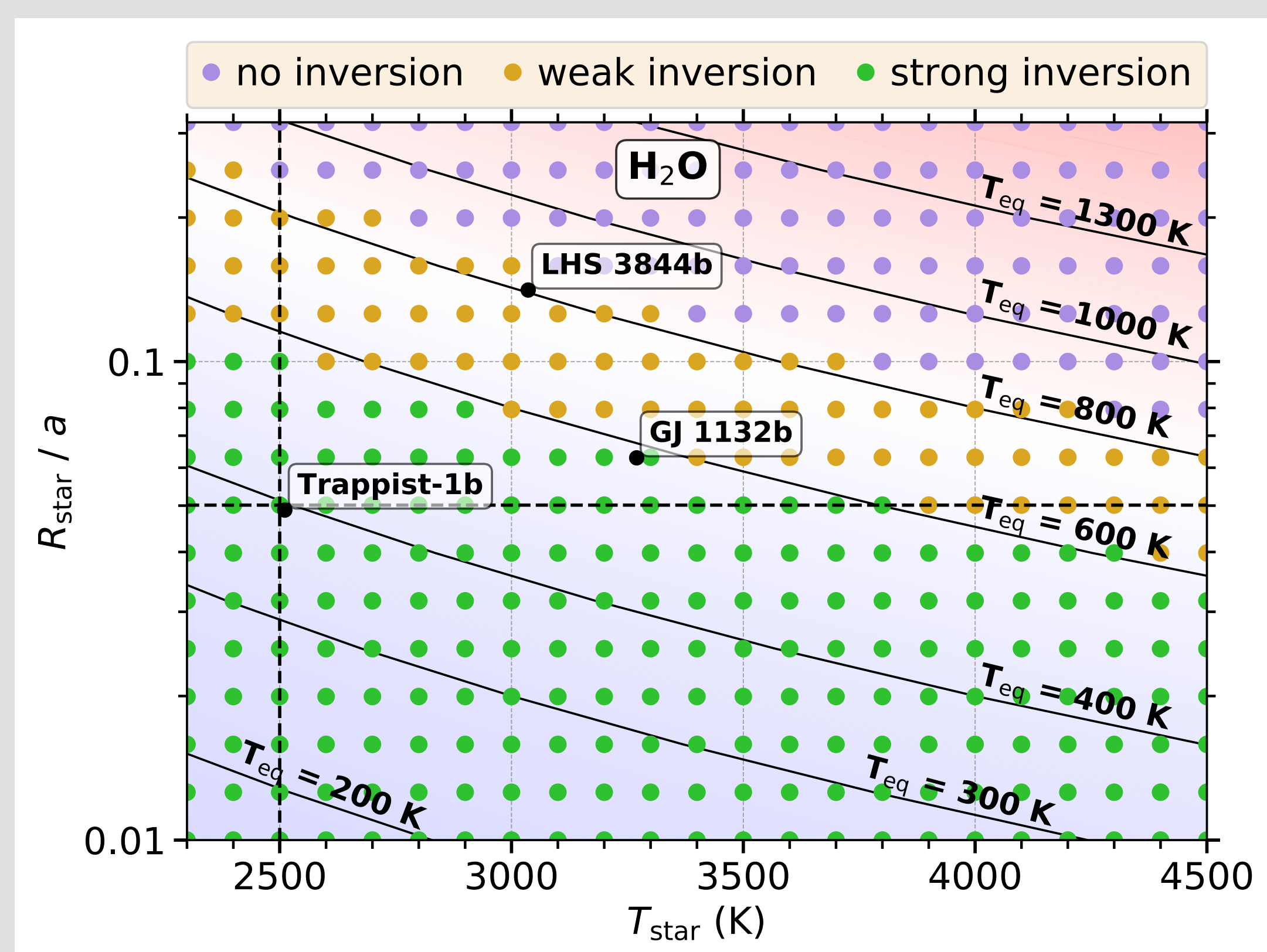


Figure 1: Presence/absence of a thermal inversion as a function of stellar temperature and radius for a pure H₂O atmosphere. Solid black lines show equilibrium temperature contours assuming a Bond albedo of 0.1. Labeled points show the locations of the three planets we study. Figure from [7].

References

- [1] Tian, F. 2009, ApJ, 703, 905. [2] Berta-Thompson, Z. K. et al. 2015, Nature, 527, 204. [3] Gillon, M. et al. 2017, Nature, 542, 456. [4] Vanderspek, R. et al. 2019, ApJL, 871, L24. [5] Malik, M. et al. 2017, AJ, 153, 56. [6] Malik, M. et al. 2019, arXiv:1903.06794. [7] Malik, M. et al., submitted. [8] Koll, D. D. B. submitted. [9] Koll, D. D. B. et al., submitted. [10] Batalha, N. E. et al. 2017, PASP, 129, 064501. [11] Seager, S. & Deming, D. 2009, ApJ, 703, 1884. [12] Morley, C. V. et al. 2017, ApJ, 850, 121. [13] Mansfield, M. et al., submitted. [14] Hu, R. et al. 2012, ApJ, 752, 7.

3D GCM Scalings (Koll, submitted)

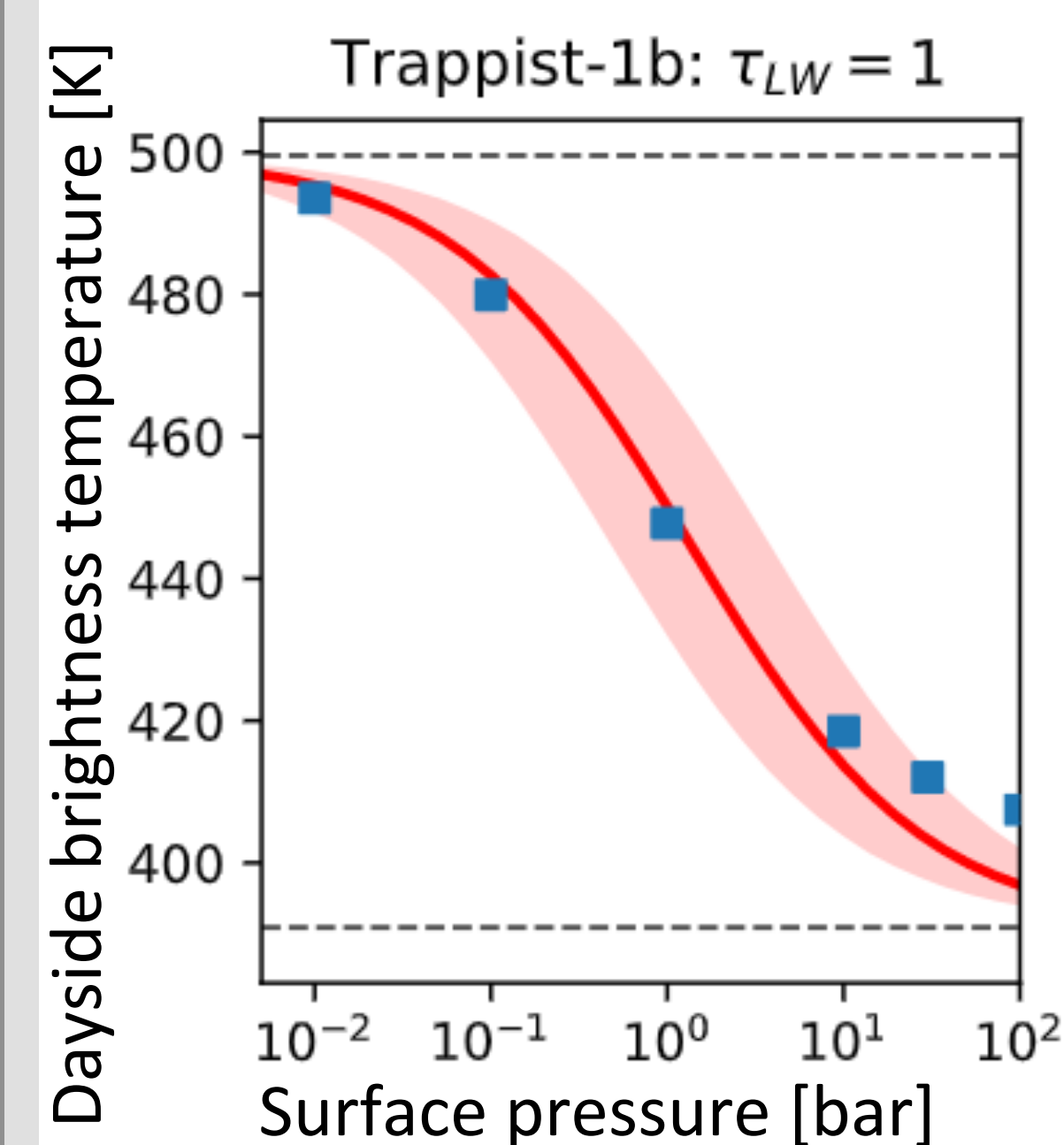


Figure 2: Comparison between GCM results (blue points) and the theoretical scaling in Eqn. 1 (red line) for a planet with the parameters of TRAPPIST-1b and $\tau_{LW}=1$. Shaded areas indicate a factor of two uncertainty in the heat engine efficiency. Dashed lines indicate limits of zero and uniform heat redistribution. Figure from [8].

- Analytical scaling for heat redistribution (f) on tidally locked rocky exoplanets

$$f = \frac{2}{3} - \frac{5}{12} \frac{\tau_{LW} (p_s)^{2/3} (T_{eq})^{-4.3}}{k + \tau_{LW} (p_s)^{2/3} (T_{eq})^{-4.3}} \quad (1)$$

where τ_{LW} =optical thickness, p_s =surface pressure [bar], T_{eq} =equilibrium temperature [K], k =constant of order unity

- Comparison to general circulation models (GCMs) shows good agreement (Fig. 2)
- Heat redistribution significantly decreases secondary eclipse depth for $P_{atm} \geq 1$ bar**

Eclipse Photometry to Find Atmospheres (Koll et al., submitted)

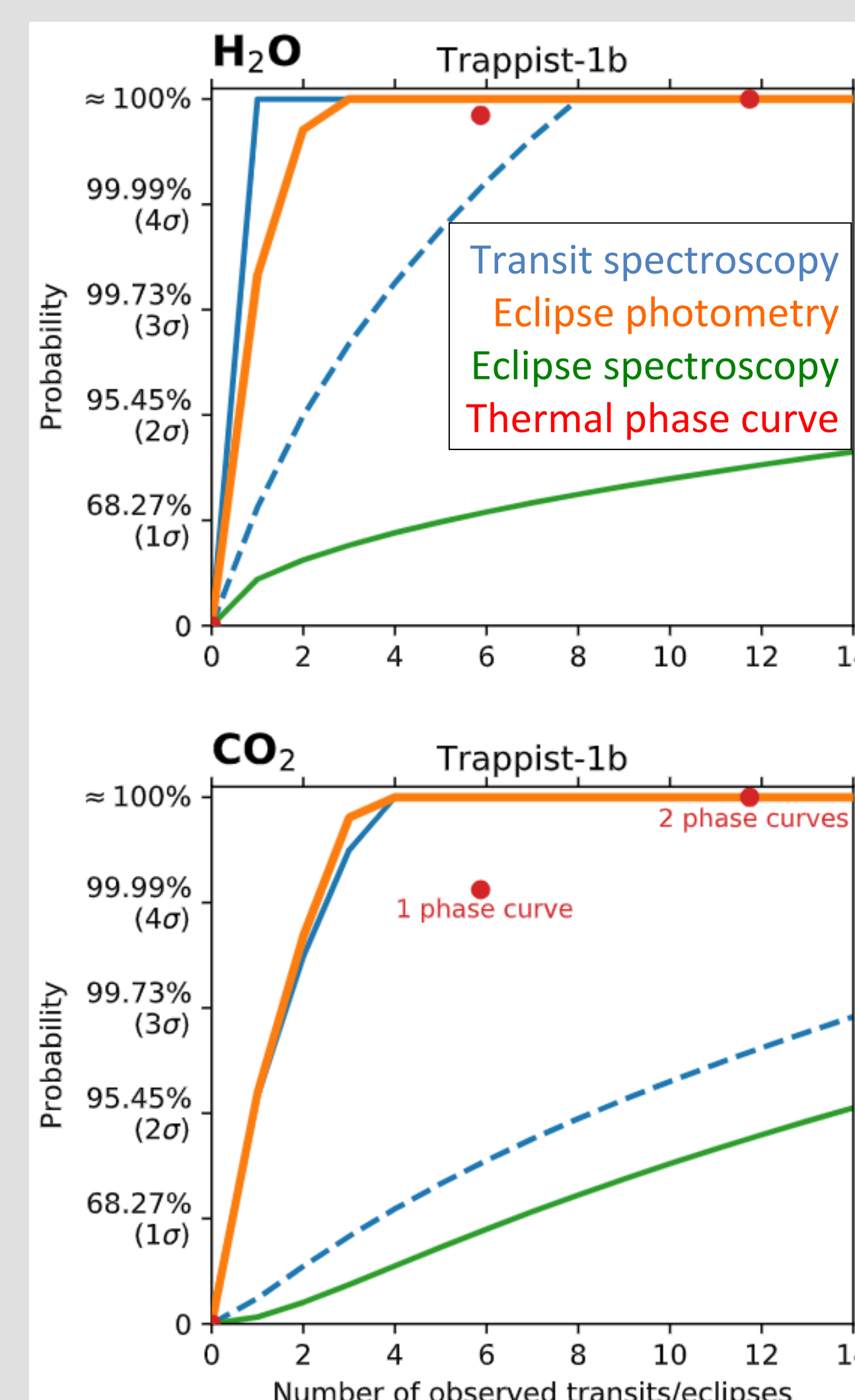


Figure 3: Number of repeated JWST observations necessary to detect a 1-bar atmosphere on TRAPPIST-1b, assuming a pure H₂O (top) or pure CO₂ (bottom) composition. For almost all cases studied, eclipse photometry (orange line) is more efficient than phase curves (red points) or transit/eclipse spectroscopy (blue/green lines), especially when considering potentially cloudy atmospheres (dashed blue line). Figure from [9].

- Lower brightness temperature → heat redistribution due to atmosphere (Fig. 5)
- Simulated JWST observations using HELIOS emission spectra [7] + heat redistribution parameterization [9]
- JWST errors simulated using PandExo [10]
- Atmosphere inferred with just 1 eclipse for $P_{atm} \geq 1$ bar**
 - More time efficient than full phase curve [11] or transit/eclipse spectroscopy [12] (Fig. 3)
 - Best follow-up method to confirm atmosphere depends on star/planet parameters

Inferred Low Albedo to Find Atmospheres (Mansfield et al., submitted)

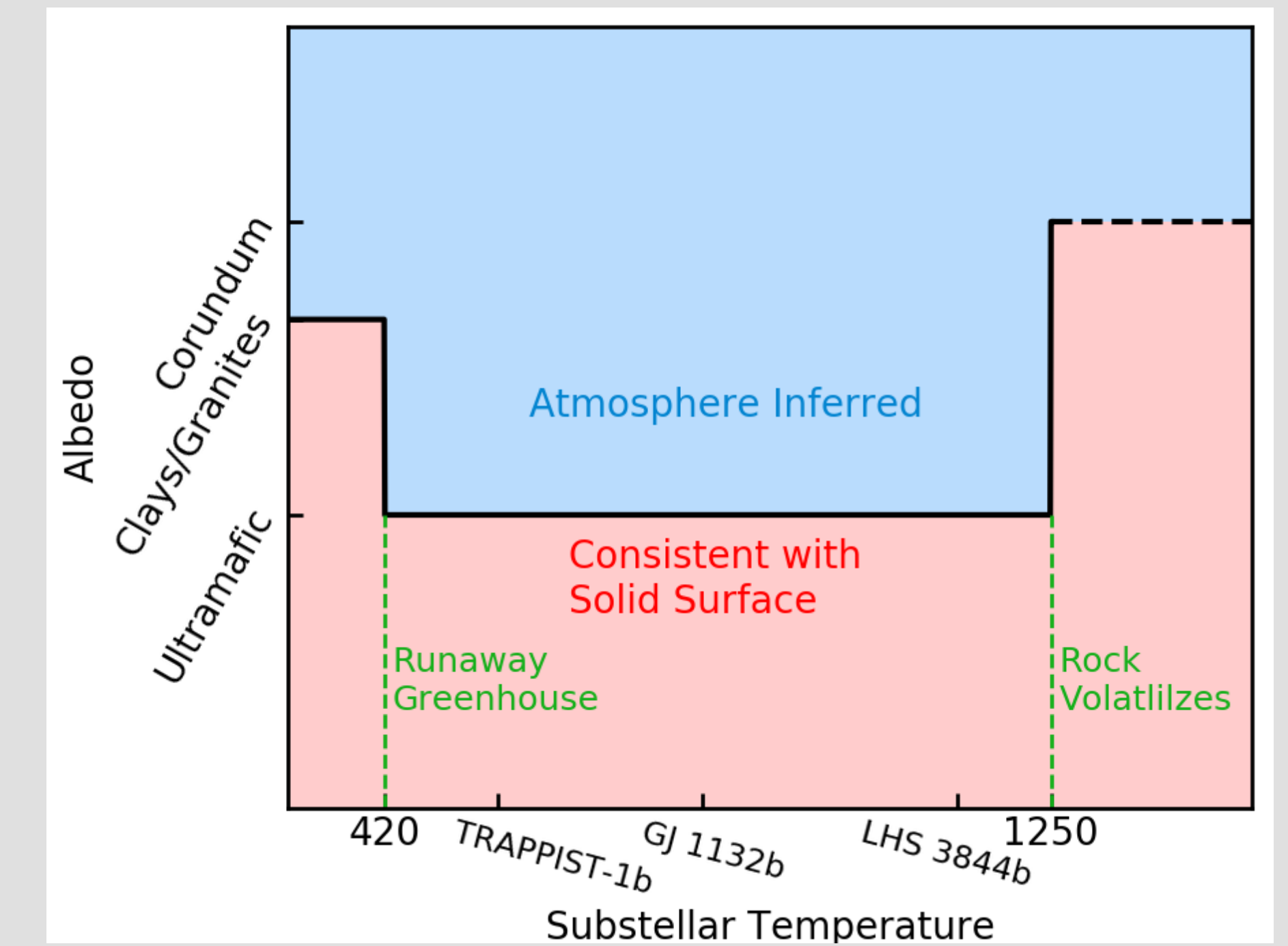


Figure 4: Substellar temperature limits within which all plausible surfaces will have low albedos. Below $T=420$ K (the runaway greenhouse limit), high-albedo, water-rich clays and granites may exist. Above $T=1250$ K, partial rock devolatilization leaves behind high-albedo corundum. Between these limits, a high inferred albedo implies an atmosphere. Temperatures of our three key planets are indicated. Figure from [13].

- Thin atmosphere with high-albedo clouds distinguishable from low-albedo rock (Fig. 5)**
 - For substellar $T=420-1250$ K, only expected rock surfaces have albedo < 0.2 (Fig. 4)
- Bare-rock observations simulated using 8 types of surface reflectance spectra [13]
- Simulated JWST+MIRI observations using PandExo [10] to infer planetary Bond albedo from emission
- Mie scattering calculations → clouds with optical depth $\tau > 3-6$ are higher albedo than bare rock

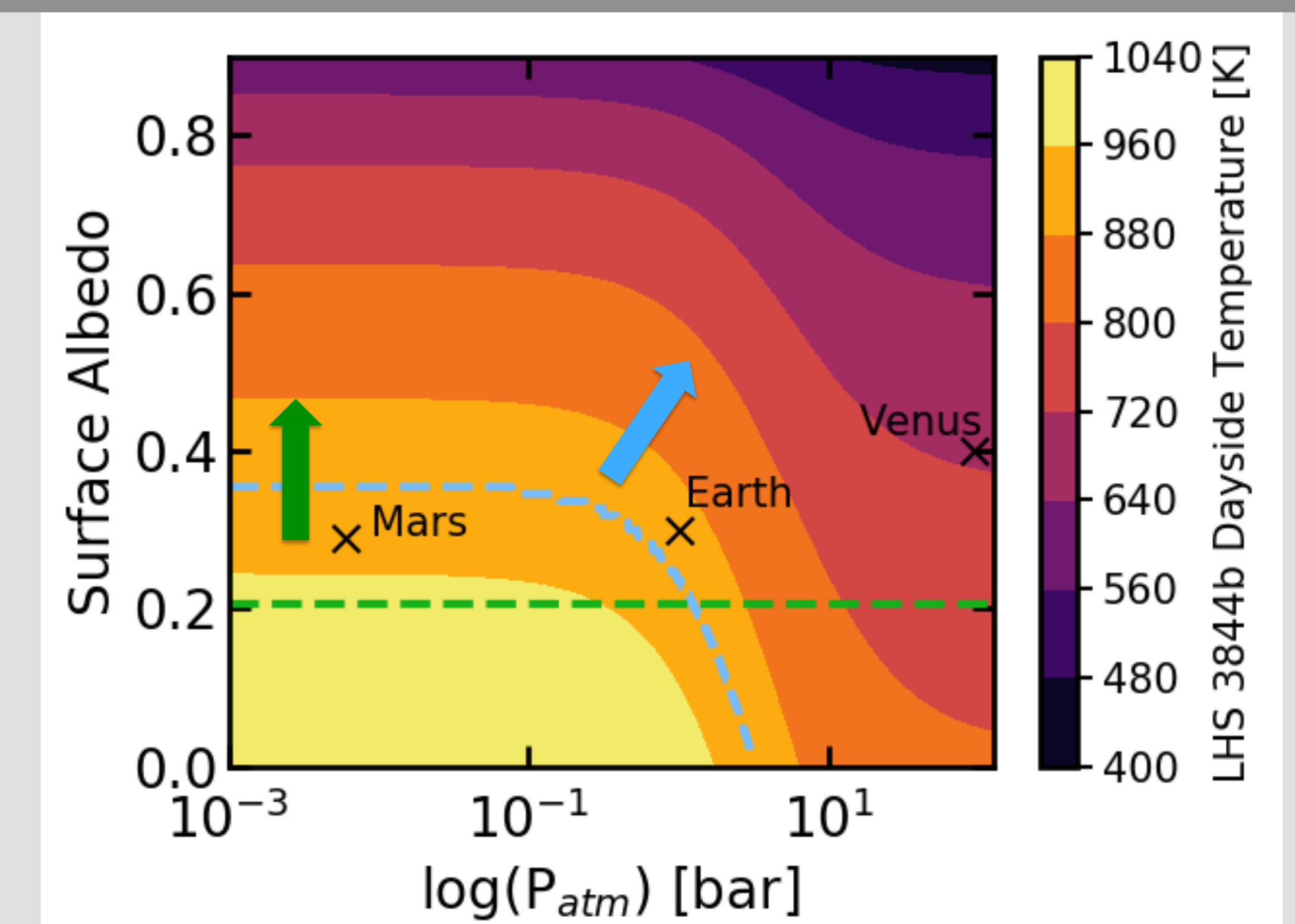


Figure 5: Relationship between the two methods of detecting an atmosphere we explore. Colored contours indicate planet dayside temperatures for LHS 3844b as a function of atmospheric pressure and surface albedos [8]. Black x marks indicate P_{atm} and albedo for Solar System planets. Eclipse photometry [9] can detect an atmosphere which decreases the dayside temperature by more than a given amount (above blue dashed line). Inferred albedo calculations [13] can detect atmospheres with albedos above a given value (above green dashed line). Figure from [13].

Questions? Come ask me!
meganmansfield@uchicago.edu

